The Astrophysical Journal, 631:429–434, 2005 September 20

VARIABILITIES OF GAMMA-RAY BURST AFTERGLOWS: LONG-ACTING ENGINE, ANISOTROPIC JET, OR MANY FLUCTUATING REGIONS?

Kunihito Ioka,[1] Shiho Kobayashi,[2] and Bing Zhang[3]
Received 2004 September 15; accepted 2005 June 6

ABSTRACT

We show that simple kinematic arguments can give limits on the timescale and amplitude of variabilities in gamma-ray burst (GRB) afterglows, especially when the variability timescale is shorter than the observed time since the burst, $\Delta t < t$. These limits help us to identify the sources of afterglow variability. The afterglows of GRB 011211 and GRB 021004 marginally violate these limits. If such violation is confirmed by the *Swift* satellite, a possible explanation is that (1) the compact objects that power GRB jets continue to eject an intermittent outflow for a very long timescale ($\gtrsim 1$ day), (2) the GRB jet from the central engine has a temporal anisotropy with a large brightness contrast $\gtrsim 10$ and small angular structure $\lesssim 10^{-2}$, or (3) many ($\gtrsim 10^3$) regions fluctuate simultaneously in the emitting site.

Subject headings: gamma rays: bursts — gamma rays: theory — relativity

1. INTRODUCTION AND SUMMARY

The standard synchrotron shock model has been successful in explaining overall features of the gamma-ray burst (GRB) afterglows (e.g., Zhang & Mészáros 2004; Mészáros 2002). The standard afterglow model assumes a single relativistic blast wave expanding into an ambient medium with a spherical, smooth density distribution. The emitting surface (shock front) is assumed to be homogeneous and spherical. Such a model predicts smooth afterglow light curves.

However, recent dense monitoring of afterglow light curves indicates that at least some afterglows deviate from a smooth power-law decay, such as in GRB 021004 (e.g., Lazzati et al. 2002; Kobayashi & Zhang 2003; Fox et al. 2003; Heyl & Perna 2003; Nakar et al. 2003) and GRB 030329 (e.g., Uemura et al. 2003; Lipkin et al. 2004; Torii et al. 2003; Sato et al. 2003; Urata et al. 2004). In addition, short-term variabilities (with the variability timescale Δt shorter than the observed time since the burst t) are observed in the afterglows of GRB 011211 (Jakobsson et al. 2004; Holland et al. 2002) and GRB 021004 (Bersier et al. 2003; Halpern et al. 2002). These variabilities carry a wealth of information about the central engine and its surroundings.

Thus far, four major scenarios have been proposed for afterglow variabilities: (1) The ambient density into which a blast wave expands may have fluctuations (see § 3.1). (2) The emitting surface might have an intrinsic angular structure, i.e., the so-called patchy shell model (see § 3.2). (3) The shocks might be "refreshed" by slow shells that catch up with the decelerated leading shell (see § 3.3). (4) The central engine might still be active at the observing time (see § 3.4).

In this paper, we show that some kinds of afterglow variability are kinematically forbidden under some standard assumptions. We assume that the standard model determines the power-law baseline of the afterglow flux F_ν and derive the following limits for dips (bumps) that deviate below (above) the baseline with a timescale Δt and amplitude ΔF_ν:

(*a*) No dips in afterglow light curves can have a larger amplitude than the limit given by equation (4) (see § 2).

(*b*) Ambient density fluctuations cannot make a bump in afterglow light curves larger than that in equation (7) (see § 3.1).

(*c*) Patchy shells cannot make a bump with a timescale shorter than the observed time $\Delta t < t$, although the rising time $\Delta t_{\rm rise} < t$ is allowed (see § 3.2).

(*d*) Refreshed shocks cannot make a bump with $\Delta t < t/4$ (see § 3.3).

These limits are summarized in Figure 1. Notice that limits *c* and *d* are derived from purely geometrical arguments, and hence, they only give constraints on Δt (not on ΔF_ν). When many regions fluctuate simultaneously, limits *a* and *b* are modified and are given by equations (A1) and (A2), respectively, as discussed in the Appendix.

The observed variabilities in the afterglows of GRB 011211 (Jakobsson et al. 2004; Holland et al. 2002) and GRB 021004 (Bersier et al. 2003; Halpern et al. 2002) might actually violate all the above limits *a*–*d*, although these are still within errors. We suggest[4] that this might imply that

1. the central engine is still active at the observed time ($\gtrsim 1$ day; see § 3.4),
2. the GRB jets have a temporal anisotropy with a small angular structure and large brightness contrast (eqs. [9] and [10] in § 4),
3. or many ($\gtrsim 10^3$) regions fluctuate simultaneously in the emitting site (see Appendix).

Therefore, variabilities in afterglow light curves can provide important clues to the nature of the compact object that triggers the burst and its surroundings. The *Swift* satellite will significantly increase such samples, and it will allow us to further understand the nature of GRB engines.

2. DIPS IN AFTERGLOW LIGHT CURVES

First let us consider dips in afterglow light curves at which the flux temporarily decreases below the expected power-law decay

[1] Physics Department and Center for Gravitational Wave Physics, 104 Davey Laboratory, Pennsylvania State University, University Park, PA 16802.
[2] Department of Astronomy and Astrophysics, 525 Davey Laboratory, Pennsylvania State University, University Park, PA 16802.
[3] Department of Physics, University of Nevada, Las Vegas, NV 89154.

[4] Jakobsson et al. (2004) have also suggested the long-acting engine and the asymmetric density or energy variations as the origin of the variabilities observed in GRB 011211 through geometrical considerations.

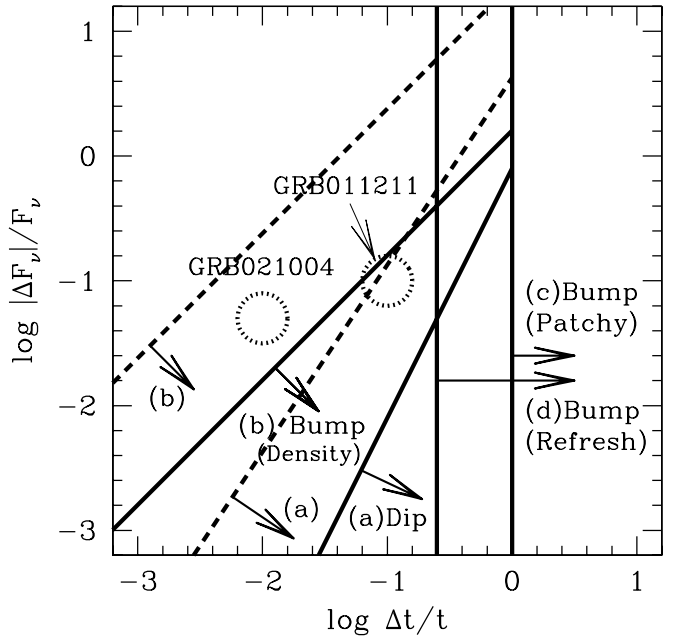

FIG. 1.—Kinematically allowed regions for afterglow variabilities shown in the plane of the relative variability timescale $\Delta t/t$ and relative variability flux $\Delta F_\nu/F_\nu$. We have four limits: (*a*) eq. (4) for dips, (*b*) eq. (7) for bumps due to density fluctuations, (*c*) $\Delta t \geq t$ for bumps due to patchy shells, and (*d*) $\Delta t \geq t/4$ for bumps due to refreshed shocks. For limits *a* and *b*, the on-axis cases are shown. When many regions fluctuate simultaneously, limits *a* and *b* are replaced by eqs. (A1) and (A2), respectively, and the off-axis cases are shown by dashed lines. We assume $F/\nu F_\nu \sim 1$ and $f_c \sim \frac{1}{2}$. The variabilities in the afterglows of GRB 011211 (Jakobsson et al. 2004; Holland et al. 2002) and GRB 021004 (Bersier et al. 2003; Halpern et al. 2002) are also shown by dotted circles and might violate some of these limits.

with a duration Δt smaller than the observing time t, i.e., $\Delta t \leq t$. We assume that dips arise from nonuniformity on the emitting surface induced by a certain mechanism (e.g., density fluctuations). Because of the relativistic beaming, the visible half-angular size of an emitting surface with a Lorentz factor γ is about γ^{-1}. Since the emitting surface with a radius $\sim R$ has a curvature, two photons emitted on the line of sight and at the edge of the visible surface travel in different times to the observer. This angular spreading time mainly determines the observed time since the burst, i.e., $t \sim R/2\gamma^2 c$ (Fenimore et al. 1996; Sari & Piran 1997). If a variable region has a half-angular size $\Delta\theta(\leq\gamma^{-1})$ and a viewing angle (with respect to the center of the variable region) $\theta_v(\leq\gamma^{-1})$ to the observer, the angular spreading effect also puts a lower limit on the variable timescale[5] as $\Delta t \geq R\Delta\theta \max(\Delta\theta/2,\ 2\theta_v)/c$. (This does not depend on the Lorentz factor of the variable region.) Then the ratio of the variable area $\Delta S \sim \pi(R\Delta\theta)^2$ to the visible area $S \sim \pi(R/\gamma)^2$ has an upper limit,

$$\frac{\Delta S}{S} \sim (\gamma\Delta\theta)^2 \leq \begin{cases} \dfrac{\Delta t}{t}, & \text{on-axis,} \\ \dfrac{1}{4}\left(\dfrac{\Delta t}{t}\right)^2, & \text{off-axis,} \end{cases} \tag{1}$$

where we use the typical value $\theta_v \sim \gamma^{-1}/2$ for the off-axis case $\theta_v \gtrsim \Delta\theta$.

In addition, the thickness of the blast wave affected by a certain mechanism (e.g., density fluctuations) should be less than the variability timescale multiplied by the speed of light $\sim c\Delta t$. Since the overall thickness of the blast wave is about $\sim R/16\gamma^2 \sim ct/8$, the ratio of the variable volume $\Delta V \sim c\Delta t\Delta S$ to the visible volume $V \sim ctS/8$ is less than

$$\frac{\Delta V}{V} \leq \begin{cases} 8\left(\dfrac{\Delta t}{t}\right)^2, & \text{on-axis,} \\ 2\left(\dfrac{\Delta t}{t}\right)^3, & \text{off-axis.} \end{cases} \tag{2}$$

To obtain the upper limits on the amplitude of a dip, we assume that the emission from the variable volume is suddenly shut off. Additional effects (e.g., cooling timescale) only make the dip less significant. Then the kinematical upper limits for the dips are

$$\frac{|\Delta F_\nu|}{F_\nu} \leq \frac{\Delta V}{V} \leq \begin{cases} 8\left(\dfrac{\Delta t}{t}\right)^2, & \text{on-axis,} \\ 2\left(\dfrac{\Delta t}{t}\right)^3, & \text{off-axis,} \end{cases} \tag{3}$$

regardless of the cause of the variability, as long as the dips are produced by a disturbance on the emitting surface.

When deriving equation (3) from equation (2), we assumed that the visible region has a uniform brightness. In reality, a spherical afterglow appears on the sky as a ring because of the relativistic effect (Panaitescu & Mészáros 1998; Sari 1998; Waxman 1997). Since the surface brightness normalized by its mean value is about $I_\nu/\bar{I}_\nu \sim 0.1$ at the center and about $I_\nu/\bar{I}_\nu \sim 3$ at the edge in the optical band ($F_\nu \propto \nu^{(1-p)/2}$) even for a uniform surface (Granot & Loeb 2001), we replace equation (3) by

$$\frac{|\Delta F_\nu|}{F_\nu} \leq \begin{cases} \dfrac{4}{5}\left(\dfrac{\Delta t}{t}\right)^2, & \text{on-axis,} \\ 6\left(\dfrac{\Delta t}{t}\right)^3, & \text{off-axis.} \end{cases} \tag{4}$$

The above limit is applicable when the emitting surface has one single variable region. When many regions fluctuate simultaneously, one can use equation (A1) instead, as discussed in the Appendix. Notice, however, that the limit in equation (4) is still useful, since its violation implies that there are many variable regions.

3. BUMPS IN AFTERGLOW LIGHT CURVES

Since the surface brightness of variable regions has a lower limit (zero), we could give constraints on dips in a general way. However, when considering afterglow bumps, since the surface brightness of variable regions has no upper limit in principle, its constraint should depend on the specific model of bumps. In the following we separately discuss each probable scenario in turn.

3.1. *Ambient Density Fluctuations*

Ambient density fluctuations can lead to afterglow variabilities (Wang & Loeb 2000; Lazzati et al. 2002; Dai & Lu 2002; Nakar et al. 2003). Such fluctuations might be due to turbulence of the interstellar medium or variable winds from the progenitor star. Here we obtain a kinematical upper limit on the variabilities that does not depend on the properties of the density fluctuations.

As in the case of dips, which we have discussed in the previous section, the ratio of the variable volume ΔV to the visible volume V satisfies equation (2). Since the kinetic energy in the

[5] Note that $\Delta t \geq R[(\theta_v + \Delta\theta)^2 - (\theta_v - \Delta\theta)^2]/2c = 2R\Delta\theta\theta_v/c$ for the off-axis case.

visible volume $E_{\rm kin}$ is almost uniformly distributed and the conversion efficiency from the kinetic energy $E_{\rm kin}$ to the internal energy E (lab frame) by shocks is close to unity (i.e., $E \sim E_{\rm kin}$) if the shocks are relativistic, we have $\Delta E/E \lesssim \Delta E_{\rm kin}/E_{\rm kin} \sim \Delta V/V$, where ΔE ($\lesssim \Delta E_{\rm kin}$) is the internal (lab frame) energy to produce the variability. Therefore, the bolometric luminosity ratio of the variable part ΔL to the base level L is less than

$$\frac{\Delta L}{L} \le \frac{\Delta E/\Delta t}{f_c E/t} \le \begin{cases} 8 f_c^{-1} \dfrac{\Delta t}{t}, & \text{on-axis,} \\ 2 f_c^{-1} \left(\dfrac{\Delta t}{t}\right)^2, & \text{off-axis,} \end{cases} \tag{5}$$

where we assume $L \sim \epsilon_e f_c E/t$, which is a good approximation for the standard afterglow, and $\Delta L \le \epsilon_e \Delta E/\Delta t$, which does not depend on the precise radiative process.[6] The fraction of cooling energy is about $f_c \sim (\nu_m/\nu_c)^{(p-2)/2} \sim \frac{1}{2}$ for the typical standard afterglow, i.e., the cooling frequency $\nu_c \sim 10^{15}$ Hz, the characteristic synchrotron frequency $\nu_m \sim 10^{12}$ Hz, and the electron power-law distribution index $p \sim 2.2$ (Sari et al. 1998).

Since the variable flux $\nu \Delta F_\nu$ at an observed frequency ν is clearly less than the bolometric variable flux ΔF (i.e., $\nu \Delta F_\nu \le \Delta F$), we can put the upper limits on bumps due to density fluctuations as

$$\frac{\Delta F_\nu}{F_\nu} \le \frac{F}{\nu F_\nu}\frac{\Delta F}{F} \le \begin{cases} 8 f_c^{-1} \dfrac{F}{\nu F_\nu}\dfrac{\Delta t}{t}, & \text{on-axis,} \\ 2 f_c^{-1} \dfrac{F}{\nu F_\nu}\left(\dfrac{\Delta t}{t}\right)^2, & \text{off-axis,} \end{cases} \tag{6}$$

where F is the bolometric base flux. The second inequality in equation (6) was derived by using $\Delta F/F \le \Delta L/L$ and equation (5). This is because the bolometric flux F (ΔF) is proportional to the luminosity L (ΔL) divided by the solid angle into which the emission is beamed, and the density enhancement only decelerates the emitting matter to reduce the relativistic beaming.[7] We can estimate the factor $F/\nu F_\nu$ in equation (6) assuming the standard afterglow model as $F/\nu F_\nu \sim (\nu/\nu_c)^{(p-3)/2}$ for $\nu_m < \nu < \nu_c$ (the optical band at $t \sim 1$ day) and $F/\nu F_\nu \sim (\nu/\nu_c)^{(p-2)/2}$ for $\nu_m < \nu_c < \nu$ (the X-ray band at $t \sim 1$ day), since the synchrotron flux $\nu_c F_{\nu_c}$ at the cooling frequency ν_c is about the bolometric flux F for $p \sim 2.2$ (Sari et al. 1998). Since $\nu_c \sim 10^{15}$ Hz at $t \sim 1$ day, we have $F/\nu F_\nu \sim 1$ for the optical and X-ray bands ($\nu \gtrsim 10^{15}$ Hz).

Finally, taking the ringlike image of the afterglow into account as in equation (4), we replace equation (6) by

$$\frac{\Delta F_\nu}{F_\nu} \le \begin{cases} \dfrac{4}{5} f_c^{-1} \dfrac{F}{\nu F_\nu}\dfrac{\Delta t}{t}, & \text{on-axis,} \\ 6 f_c^{-1} \dfrac{F}{\nu F_\nu}\left(\dfrac{\Delta t}{t}\right)^2, & \text{off-axis.} \end{cases} \tag{7}$$

Note that the above derivation uses only the properties of the standard afterglow.

The above limit can be applied when the emitting site has a single variable region. When many regions fluctuate simultaneously, we can use equation (A2) instead, as discussed in the Appendix. Note, however, that the limit in equation (7) is still useful, since its violation implies many variable regions.

3.2. *Patchy Shell Model*

An intrinsic angular structure on the emitting surface (patchy shell) can also produce the variability of the afterglow (Mészáros et al. 1998; Kumar & Piran 2000b). Such patchy shells can be realized in the subjet model (Yamazaki et al. 2004; Ioka & Nakamura 2001a). Since the visible size $\sim\gamma^{-1}$ grows as the Lorentz factor γ drops, the observed flux varies depending on the angular structure.

The variability timescale is always $\Delta t \ge t$ (Nakar & Oren 2004) if the angular fluctuation is persistent (see also § 4). The rise time of the variability $\Delta t_{\rm rise}$ could be $\Delta t_{\rm rise}/t \sim 2\gamma\Delta\theta < 1$, since it is determined by the timescale on which the angular fluctuation $\Delta\theta$ enters the visible region. (The lateral expansion has to be slow for $\Delta\theta < \gamma^{-1}$; see § 4.) However, it takes $\sim t$ for the flux to go back to its mean level, since the visible region expands on the timescale $\sim t$.

3.3. *Refreshed Shocks*

Afterglow variabilities can also arise in the refreshed shock scenario, in which multiple shells are ejected instantaneously (i.e., the ejection timescale is comparable to the GRB duration and short compared to the observed time), but the inner shell is so slow that it catches up with the outer shells on a long timescale when the Lorentz factor of the outer shells drops slightly below that of the slow shell (Rees & Mészáros 1998; Panaitescu et al. 1998; Kumar & Piran 2000a; Sari & Mészáros 2000; Zhang & Mészáros 2002). Since inner shells only increase the afterglow energy, the observed flux does not go back to the original level (i.e., the extrapolation from the original power law).

The variability timescale should be $\Delta t \ge t/4$ if the acceleration of the GRB ejecta is hydrodynamic. This is because, if hydrodynamically accelerated, the slow shell has an opening angle larger than the inverse of its Lorentz factor $\Delta\theta \ge \gamma_s^{-1}$ and a factor of $\sim$2 dispersion in the Lorentz factor of the slow shell γ_s, since the shell is hot in the acceleration regime and expands with a sound speed $\sim c$ in the comoving frame. If $\Delta\theta \ge \gamma_s^{-1}$, the variability timescale is equal to or larger than the observed time (angular spreading time) $\Delta t \ge R/2c\gamma_s^2 \sim t/4$, since the Lorentz factor of the slow shell is comparable to that of the blast wave $\gamma_s \sim 2\gamma$ when they collide. Even when $\Delta\theta < \gamma_s^{-1}$, if the Lorentz factor of the slow shell γ_s varies at least by a factor of $\sim$2, the slow shell spreads to have a width in the lab-frame $\Delta \sim R/2\gamma_s^2 \sim ct/4$, so the variability timescale is again $\Delta t \ge t/4$. Therefore, another acceleration mechanism is required for $\Delta t < t/4$.

The slow shell might satisfy $\Delta\theta < \gamma_s^{-1}$ if the outer shell has an opening angle smaller than γ_s^{-1}. This is because a part of the slow shell outside the wake of the outer shell is decelerated and cut off by the ambient material. Only the shell in the wake remains cold and freely expands. This mechanism might explain the bumps in GRB 030329 with $\Delta t \sim t_j < t$, where t_j is the jet break time (Granot et al. 2003). However, the dispersion of γ_s should be small for $\Delta \le c\Delta t$, so a nonhydrodynamic acceleration is still needed.

3.4. *Long-Acting Engine Model*

A bump at an observed time t might suggest that the central engine is still active at that time t (Rees & Mészáros 2000; Zhang & Mészáros 2002; Dai & Lu 1998). A very long duration could arise if it takes a long time for the disk around a black hole to be completely absorbed, such as in some cases of the collapsar

[6] We implicitly assume that the energy fraction that goes into electrons ϵ_e is determined by the microscopic physics and is constant.

[7] If we consider a void in the ambient medium, instead of the density enhancement, the matter freely expands in the void, so that the Lorentz factor becomes higher than that in other parts. However, the difference within $\Delta t \le t$ is only a factor of $\sim$2 and negligible for an order-of-magnitude argument.

models (e.g., MacFadyen et al. 2001) or if the central object becomes a neutron star, such as a millisecond magnetar (e.g., Usov 1994).

Afterglow variabilities might arise when a long-term intermittent outflow from the central engine collides with the preceding blast wave,[8] with itself (internal shock), or with the progenitor stellar envelope. In principle, the variability timescale could be down to the millisecond level (light crossing time of the central engine) and there is no limit on the flux variability. The minimum energy to produce the variability is

$$\frac{\Delta E}{E} \geq \frac{\nu F_\nu}{F} \frac{\Delta F_\nu}{F_\nu} \frac{\Delta t}{t} \frac{\Omega}{\pi \gamma^{-2}}, \tag{8}$$

where Ω is the solid angle into which the variable emission is collimated and E is the afterglow energy in the visible region. Since the solid angle Ω can be as low as $\sim \pi \gamma_v^{-2}$, the inverse square of the Lorentz factor of the emitting matter, there is in principle no lower limit for Ω, and hence for the minimum energy ΔE, if we consider a high Lorentz factor γ_v. Considering other effects (such as multishock emission upon collision) might require a larger energy (Zhang & Mészáros 2002).

High-energy gamma rays could be a diagnosis of the model (Ramirez-Ruiz 2004).

3.5. *Others*

There are several other possibilities for producing variabilities in afterglow light curves: gravitational microlensing (Loeb & Perna 1998; Garnavich et al. 2000; Ioka & Nakamura 2001b), combined reverse shock and forward shock emission (Kobayashi & Zhang 2003), supernova bumps (e.g., Bloom et al. 1999), and dust echoes (Esin & Blandford 2000; Mészáros & Gruzinov 2000). These are not repeated, and the variability timescales are usually $\Delta t/t \gtrsim 0.1$. Since these variabilities have distinct temporal and spectral features, we will be able to distinguish these possibilities from the mechanisms we have discussed in this paper.

4. SOLUTIONS TO FORBIDDEN VARIABILITIES

We have studied kinematical limits on the afterglow variabilities for both dips and bumps, which are summarized in Figure 1: (*a*) dips have a smaller amplitude than that given by equation (4); (*b*) density fluctuations cannot make a bump larger than the limit of equation (7); (*c*) patchy shells cannot make a bump with a timescale shorter than the observed time $\Delta t < t$; and (*d*) refreshed shocks cannot make a bump with $\Delta t < t/4$. If many regions fluctuate simultaneously, limits *a* and *b* are replaced by equations (A1) and (A2), respectively, as discussed in the Appendix. The variabilities in GRB 011211 ($\Delta t/t \sim 0.1$ and $|\Delta F_\nu|/F_\nu \sim 0.1$; Jakobsson et al. 2004; Holland et al. 2002) might violate limits *a*, *c*, and *d* and marginally violate *b*, while the variabilities in GRB 021004 ($\Delta t/t \sim 0.01$ and $|\Delta F_\nu|/F_\nu \sim 0.05$; Bersier et al. 2003; Halpern et al. 2002) might violate all these limits, if a single region fluctuates, although still within errors.

1. One possible explanation for the forbidden variabilities is the day-long central engine model discussed in § 3.4. Interestingly, this scenario could easily produce metal features (Rees & Mészáros 2000) and the metal emission lines are indeed observed in the X-ray afterglow of GRB 011211 (Reeves et al. 2002). A simple form of this model can explain forbidden bumps but not dips. Nevertheless, as noted by Rees & Mészáros (2000), we cannot rule out the possibility that all afterglow is due to the central engine itself. This extreme version of this model might resolve the forbidden bumps, as well as dips in the afterglow.

2. Another solution could be provided by nonstandard assumptions that the emitting surface is anisotropic (during the period when light curves smoothly decay) and that the anisotropy is temporal.[9] Since equation (1) is derived from geometrical arguments and applicable to both dips and bumps, the angular size of the anisotropy needs to be

$$\Delta\theta \leq \begin{cases} \gamma^{-1} \left(\dfrac{\Delta t}{t}\right)^{1/2} \sim 10^{-2}, & \text{on-axis,} \\ \dfrac{1}{2}\gamma^{-1}\dfrac{\Delta t}{t} \sim 10^{-3}, & \text{off-axis,} \end{cases} \tag{9}$$

and with the temporal timescale $\sim \Delta t$ the surface brightness in this region should be enhanced (bumps) or reduced (dips) by

$$\frac{|\Delta I_\nu|}{\bar{I}_\nu} = \frac{|\Delta F_\nu|}{F_\nu}\frac{S}{\Delta S} \geq \begin{cases} \dfrac{|\Delta F_\nu|}{F_\nu}\dfrac{t}{\Delta t} \sim 10, & \text{on-axis,} \\ 4\dfrac{|\Delta F_\nu|}{F_\nu}\left(\dfrac{t}{\Delta t}\right)^2 \sim 10^3, & \text{off-axis,} \end{cases} \tag{10}$$

where numerical values are for GRB 021004 ($\Delta t/t \sim 0.01$ and $|\Delta F_\nu|/F_\nu \sim 0.05$) and we have assumed $\gamma \sim 10$ at $t \sim 1$ day. For the off-axis case, the brightness contrast might be too large, $|\Delta I_\nu|/\bar{I}_\nu \sim 10^3$, to be reconciled with the observed narrow distribution of the geometrically corrected gamma-ray energy (Frail et al. 2001).

Let us examine each violation one by one in this temporally anisotropic model. To explain narrow dips violating *a*, the variable region should be initially brighter than the limit given by equation (10) and then it should be darkened, such as by the density fluctuations. However, the angular size should also satisfy equation (9). This size is contrary to our common belief that the initial fluctuations with $\Delta\theta < \gamma^{-1}$ are erased during the fireball evolution because the visible region $\sim\gamma^{-1}$ is causally connected. The lateral expansion has to be slower than the usual assumption (i.e., the sound speed in the local frame) for the initial fluctuations to prevail. (Notice that several numerical simulations imply a slow lateral expansion; Granot et al. 2001; Kumar & Granot 2003; Cannizzo et al. 2004.) We also expect that other variabilities due to the patchy shell effect should appear in the light curves when the angular fluctuations enter the visible region.

Next let us consider bumps violating the limits *b*–*d* in the temporally anisotropic model. To explain variabilities violating limit *b* in the density fluctuation scenario, the angular energy distribution has to be initially anisotropic and the energetic spot needs to be brightened by the density fluctuation, as in the dip case *a*. Again the lateral expansion has to be slow, and we also expect other variabilities due to the patchy shell effect. In the patchy shell model violating limit *c*, the anisotropy should be temporal $\sim\Delta t$, so an external factor such as density fluctuations may be necessary. Also in this case the lateral expansion has to be slow. For the bumps due to refreshed shocks to violate limit *d*, the acceleration mechanism should be nonhydrodynamic (see § 3.3). If so, the rise time $\Delta t_{\rm rise}$ could be as short as $\Delta t_{\rm rise}/t \sim (\gamma\Delta\theta)^2 < 1$

[8] In the refreshed shock scenario (in the previous section), shells are ejected at almost the same time, not for a long time.

[9] In the patchy shell model, the anisotropy is not temporal but persistent (see § 3.2).

(on-axis), but the flux does not return to the original level. The stepwise light curve is a signature of the refreshed shock.

3. The other solution could be that many regions fluctuate simultaneously. As discussed in the Appendix, limits *a* and *b* are modified in this case and are given by equations (A1) and (A2), respectively. Limit *a* for dips in equation (A1) might still be violated by GRB 011211 and GRB 021004, while limit *b* for bumps due to density fluctuations in equation (A2) might not be violated. Even so, the number of variable regions has to be larger than $\sim 10^3$ to reconcile limit *b* with GRB 021004, and this suggests that the mean separation of the density clumps (with a radius $\sim 10^{14}$ cm) is about $\sim 10^{15}$ cm (see Appendix). Therefore, these limits provide interesting constraints on density fluctuations. In this model the anisotropy of the emitting surface is also strong and temporal as in the previous model, and the observed flux almost always differs from the base level.

4. The violations could be attributed to uncertainties of the observations and data analyses. The violation of equation (4), which gives constraints on dips, might be due to the fitting scheme, because spurious dips might be produced by inappropriate power-law fitting to a light curve containing bumps. Intensive afterglow monitorings such as those by the *Swift* satellite and its ground-based follow-up observations, when combined with appropriate data-fitting methods, might be able to lead to a better determination of the base level of the decay, which could be used to verify or refute the presence of the forbidden variabilities.

Some afterglows show small variabilities despite dense sampling (e.g., Laursen & Stanek 2003; Gorosabel et al. 2004; Stanek et al. 1999). The variety could arise from the viewing angle (e.g., the anisotropy depends on the viewing angle) or the intrinsic diversity (e.g., each burst has a different anisotropy), but future observations are needed to fix its origin.

We have considered a fixed lab-frame time to relate the emitting area and volume with the observed time in equations (1) and (2). If we take the equal arrival time surface into account (Panaitescu & Mészáros 1998; Sari 1998; Waxman 1997), these relations would be modified and make the limits more stringent especially near the limb of the afterglow image. This is also an interesting future problem.

We thank P. Mészáros, D. Lazzati, and the referee for useful comments. This work was supported in part by the Eberly Research Funds of Penn State and by the Center for Gravitational Wave Physics under grants PHY 01-14375 (for K. I. and S. K.), NASA *Swift* Cycle 1 GI Program (for S. K. and B. Z.), and NASA NNG04GD51G (for B. Z.).

APPENDIX

THE CASE OF MANY VARIABLE REGIONS

Thus far, we have considered only a single variable region to make the discussions simple. In reality, many regions could fluctuate simultaneously (e.g., Gruzinov & Waxman 1999). This leads to weaker limits for dips (*a*) and bumps due to density fluctuations (*b*) in equations (4) and (7), respectively. In any case, we can still obtain meaningful limits by extending the previous arguments, as shown below.

Let N_v be the mean number of variable regions contributing in the observed time interval of $\sim\Delta t$. Then the flux deviates from the baseline $\sim N_v$ times more than the single variable region case. However, the flux variability is determined by the differences between time intervals. This is determined by the variance of the number of variable regions from one time interval $\sim\Delta t$ to the next, and it is $\sim N_v^{1/2}$ if we assume the Poisson statistics. Poisson statistics may be applied since different variable regions fluctuate at different lab-frame times. Therefore, the limits for a single variable region in equations (4) and (7) have to be multiplied by $\sim N_v^{1/2}$ when many regions fluctuate.

A1. LIMIT *a*: DIPS

Let us consider the maximum of the number of variable regions N_v in the dip case *a*. In the on-axis case, the maximum number is about the ratio of the overall thickness of the blast wave $\sim R/16\gamma^2 \sim ct/8$ to the fluctuating thickness $\sim c\Delta t$, i.e., $N_v \le (t/\Delta t)/8$. In the off-axis case, it is about the ratio of the visible volume V to the variable volume ΔV in equation (2), i.e., $N_v \le V/\Delta V \sim (t/\Delta t)^3/2$.

Then multiplying the limits for a single variable region in equation (4) by $\sim N_v^{1/2}$, we obtain the limits for dips due to many variable regions as

$$\frac{|\Delta F_\nu|}{F_\nu} \le \begin{cases} \dfrac{\sqrt{2}}{5}\left(\dfrac{\Delta t}{t}\right)^{3/2}, & \text{on-axis,} \\ \dfrac{6}{\sqrt{2}}\left(\dfrac{\Delta t}{t}\right)^{3/2}, & \text{on-axis.} \end{cases} \tag{A1}$$

The off-axis limit is shown by the dashed line in Figure 1. The variabilities in GRB 011211 ($\Delta t/t \sim 0.1$ and $|\Delta F_\nu|/F_\nu \sim 0.1$) and GRB 021004 ($\Delta t/t \sim 0.01$ and $|\Delta F_\nu|/F_\nu \sim 0.05$) might still violate these limits.

The above limits are quite robust but might be too strict because the interior of the blast wave also needs to fluctuate at the same pace as the front and back of the blast wave when the number of variable regions N_v is nearly maximum. A reasonable fluctuating site might be the front and back of the blast wave that are affected by the density clumps or the inner shells. If this is the case, the maximum of N_v is ~ 1 in the on-axis case and is about the ratio of the visible area S to the variable area ΔS in equation (1), i.e., $N_v \le S/\Delta S \sim 4(t/\Delta t)^2$, in the off-axis case.

A2. LIMIT *b*: BUMPS DUE TO AMBIENT DENSITY FLUCTUATIONS

When the density fluctuations make bumps in the afterglow, the bumps are mainly produced at the shock front (i.e., not such as in the interior of the blast wave). Then the maximum of the number of variable regions N_v is ~ 1 in the on-axis case. In the off-axis case, it is about the ratio of the visible area S to the variable area ΔS in equation (1), i.e., $N_v \le S/\Delta S \sim 4(t/\Delta t)^2$.

Multiplying the limits for a single variable region in equation (7) by $\sim N_v^{1/2}$, we obtain the limits for bumps due to many density fluctuations as

$$\frac{\Delta F_\nu}{F_\nu} \leq \begin{cases} \frac{4}{5} f_c^{-1} \frac{F}{\nu F_\nu} \frac{\Delta t}{t}, & \text{on-axis,} \\ 12 f_c^{-1} \frac{F}{\nu F_\nu} \frac{\Delta t}{t}, & \text{off-axis.} \end{cases} \tag{A2}$$

The off-axis limit is shown by the dashed line in Figure 1. This maximum off-axis limit is not violated by the variabilities in GRB 011211 ($\Delta t/t \sim 0.1$ and $|\Delta F_\nu|/F_\nu \sim 0.1$) and GRB 021004 ($\Delta t/t \sim 0.01$ and $|\Delta F_\nu|/F_\nu \sim 0.05$). Still, we need $N_v \gtrsim 1600$ variable regions to reconcile the off-axis limit with GRB 021004 because the variabilities in GRB 021004 are $\sim 40 \sim (1600)^{1/2}$ times larger than the off-axis limit for a single variable region in equation (7). This corresponds to the mean separation of the density clumps $\sim [\pi (R/\gamma)^2 c \Delta t \gamma^2 / N_v]^{1/3} \sim 10^{15}$ cm, since the shock front with a radius $R/\gamma \sim ct\gamma \sim 10^{16}$ cm sweeps a distance $c\Delta t \gamma^2 \sim 10^{15}$ cm for $t \sim 1$ day, $\Delta t \sim 10^3$ s, and $\gamma \sim 10$. Note that we can also estimate the clump radius as $c\Delta t \gamma \sim 10^{14}$ cm. In this way, the limits in equations (7) and (A2) can impose interesting constraints on the density fluctuations.

REFERENCES

Bersier, D., et al. 2003, ApJ, 584, L43
Bloom, J. S., et al. 1999, Nature, 401, 453
Cannizzo, J. K., Gehrels, N., & Vishniac, E. T. 2004, ApJ, 601, 380
Dai, Z. G., & Lu, T. 1998, A&A, 333, L87
———. 2002, ApJ, 565, L87
Esin, A. A., & Blandford, R. 2000, ApJ, 534, L151
Fenimore, E. E., Madras, C. D., & Nayakshin, S. 1996, ApJ, 473, 998
Fox, D. W., et al. 2003, Nature, 422, 284
Frail, D. A., et al. 2001, ApJ, 562, L55
Garnavich, R. M., Loeb, A., & Stanek, K. Z. 2000, ApJ, 544, L11
Gorosabel, J., et al. 2004, A&A, 422, 113
Granot, J., & Loeb, A. 2001, ApJ, 551, L63
Granot, J., Miller, M., Piran, T., Suen, W. M., & Hughes, P. A. 2001, in GRBs in the Afterglow Era, ed. E. Costa, F. Frontera, & J. Hjorth (Berlin: Springer), 312
Granot, J., Nakar, E., & Piran, T. 2003, Nature, 426, 138
Gruzinov, A., & Waxman, E. 1999, ApJ, 511, 852
Halpern, J. P., Armstrong, E. K., Espaillat, C. C., & Kemp, J. 2002, GCN Circ. 1578, http://gcn.gsfc.nasa.gov/gcn3/1578.gcn3
Heyl, J. S., & Perna, R. 2003, ApJ, 586, L13
Holland, S. T., et al. 2002, AJ, 124, 639
Ioka, K., & Nakamura, T. 2001a, ApJ, 554, L163
———. 2001b, ApJ, 561, 703
Jakobsson, P., et al. 2004, NewA, 9, 435
Kobayashi, S., & Zhang, B. 2003, ApJ, 582, L75
Kumar, P., & Granot, J. 2003, ApJ, 591, 1075
Kumar, P., & Piran, T. 2000a, ApJ, 532, 286
———. 2000b, ApJ, 535, 152
Laursen, L. T., & Stanek, K. Z. 2003, ApJ, 597, L107
Lazzati, D., Rossi, E., Covino, S., Ghisellini, G., & Malesani, D. 2002, A&A, 396, L5
Lipkin, Y. M., et al. 2004, ApJ, 606, 381
Loeb, A., & Perna, R. 1998, ApJ, 495, 597
MacFadyen, A. I., Woosley, S. E., & Heger, A. 2001, ApJ, 550, 410
Mészáros, P. 2002, ARA&A, 40, 137
Mészáros, P., & Gruzinov, A. 2000, ApJ, 543, L35
Mészáros, P., Rees, M. J., & Wijers, R. A. M. J. 1998, ApJ, 499, 301
Nakar, E., & Oren, Y. 2004, ApJ, 602, L97
Nakar, E., Piran, T., & Granot, J. 2003, NewA, 8, 495
Panaitescu, A., & Mészáros, P. 1998, ApJ, 493, L31
Panaitescu, A., Mészáros, P., & Rees, M. J. 1998, ApJ, 503, 314
Ramirez-Ruiz, E. 2004, MNRAS, 349, L38
Rees, M. J., & Mészáros, P. 1998, ApJ, 496, L1
———. 2000, ApJ, 545, L73
Reeves, J. N., et al. 2002, Nature, 416, 512
Sari, R. 1998, ApJ, 494, L49
Sari, R., & Mészáros, P. 2000, ApJ, 535, L33
Sari, R., & Piran, T. 1997, ApJ, 485, 270
Sari, R., Piran, T., & Narayan, R. 1998, ApJ, 497, L17
Sato, R., Kawai, N., Suzuki, M., Yatsu, Y., Kataoka, J., Takagi, R., Yanagisawa, K., & Yamaoka, H. 2003, ApJ, 599, L9
Stanek, K. Z., Garnavich, P. M., Kaluzny, J., Pych, W., & Thompson, I. 1999, ApJ, 522, L39
Torii, K., et al. 2003, ApJ, 597, L101
Uemura, M., et al. 2003, Nature, 423, 843
Urata, Y., et al. 2004, ApJ, 601, L17
Usov, V. V. 1994, MNRAS, 267, 1035
Wang, X., & Loeb, A. 2000, ApJ, 535, 788
Waxman, E. 1997, ApJ, 491, L19
Yamazaki, R., Ioka, K., & Nakamura, T. 2004, ApJ, 607, L103
Zhang, B., & Mészáros, P. 2002, ApJ, 566, 712
———. 2004, Int. J. Mod. Phys. A, 19, 2385

Note added in proof.—After this paper was submitted, Burrows et al. (2005, Science, in press [astro-ph/0506130]) reported afterglow variabilities, so-called X-ray flares, that violate the kinematical limits. These strong, rapid X-ray flares imply the long activities of the central engines.